



Research Article

The Effect of Phase Change Temperature of Graphite Matrix Composite on Small-Scale Li-Ion Package Performance Under Square Wave Load

Mustafa Yusuf YAZICI^{1,2}

¹Samsun University, Engineering Faculty, Mechanical Engineering Department, 55420, Samsun, Türkiye

²University of Nottingham, Engineering Faculty, Mechanical Eng. Department, NG7 2RD, Nottingham, UK

Mustafa Yusuf YAZICI, ORCID No: 0000-0002-1076-9265

Corresponding author e-mail: myusuf.yazici@samsun.edu.tr

Article Info

Received: 14.09.2022

Accepted: 21.02.2023

Online August 2023

DOI:10.53433/yyufbed.1175411

Keywords

Battery,
Cooling,
Graphite matrix,
Li-ion,
PCM,
Thermal management

Abstract: An experimental study is performed to illustrate the effect of the melting temperature of graphite matrix composite with phase change materials on the performance characteristics of a small-scale li-ion package (3s2p) under dynamic/square wave load. Paraffin (RT35 and RT42) is used as a PCM. Graphite matrix is manufactured with 75 g l⁻¹ bulk density. The battery package is performed for three different configurations: free-air cooling case (reference case), and graphite matrix composites with RT35 and RT42. The experimental outputs present that graphite matrix composite has considerable potential for thermal management of the Li-ion pack. Safe operating time, discharge and energy capacity values are increased by 140%, 141% and 102% with the graphite composite with RT35 in the comparison reference case, respectively. It is observed that the melting temperature of PCM of graphite composite is of critical importance to the performance of the battery pack. For the graphite composite with RT35, operating time, discharge capacity and energy capacity values are enhanced by 6.2 %, 7 % and 10 % compared to the RT42 case, respectively.

Grafit Matris Kompozit Faz Dönüşüm Sıcaklığının Kare Dalga Yük Altındaki Küçük Ölçekli Bir Li-iyon Batarya Paketi Performansına Etkisi

Makale Bilgileri

Geliş: 14.09.2022

Kabul: 21.02.2023

Online Ağustos 2023

DOI:10.53433/yyufbed.1175411

Anahtar Kelimeler

Batarya,
FDM,
Grafit matris,
Li-iyon,
Soğutma,
Termal yönetim

Öz: Faz değiştiren malzeme (FDM) ilaveli kompozit grafit matris içerisindeki faz değiştiren malzeme erime sıcaklığının küçük ölçekli (3s2p) bir li-iyon paketi performansı üzerindeki etkileri dinamik-kare yük altında deneysel olarak incelenmiştir. FDM olarak parafin (RT35 ve RT42) kullanılmıştır. Grafite matris 75 g l⁻¹ yığın yoğunluğu ile üretilmiştir. Batarya paketi üç farklı konfigürasyon için test edilmiştir: doğal taşınım hava soğutma (referans durum) ve grafit kompozit-RT35 ve RT42. Deneysel çıktılar, grafit matris kompozitin li-iyon batarya paketinin termal yönetimi için önemli bir potansiyele sahip olduğunu ortaya koymaktadır. Referans duruma kıyasla grafit matris kompozit-RT35 ile güvenli çalışma süresinde %140, deşarj ve enerji kapasitesi değerlerinde ise %141 ve %102 oranında bir artış sağlanmıştır. Grafite matris kompozit içerisindeki FDM'lerin erime sıcaklıklarının batarya paketi performansı üzerinde kritik öneme sahip olduğu gözlenmiştir. Grafite matris kompozit-RT35 için çalışma süresi, deşarj kapasitesi ve enerji kapasitesi değerleri grafit matris kompozit-RT42 durumuna kıyasla, sırasıyla, %6, %7 ve %10 artırılmıştır.

1. Introduction

Electromobility is a global trend to avoid the threat of energy and climate crisis, and severe environmental pollution such as air and noise leading to environmental health risks. However, the battery is the key feature for spreading electromobility including cars, bikes. Li-ion battery technology has the highest potential among other options with no-memory effect, high specific power/energy density, long life cycle, high discharge voltage, low self-discharge and stable performance in the current era. Although the li-ion cell provides a considerable solution for electromobility, the operating conditions are subject to certain restrictions. Temperature is one of the key features of li-ion performance. There are two critical conditions for temperature for li-ion technology: improper operating temperature and high non-uniformity, which cause deteriorations in performance, safety and lifetime. The operating temperature should be within the restricted range of 15 °C – 35 °C for utilizing the li-ion technology more. Moreover, it is desired that the temperature gradient between cells should be kept at less than 5 °C to avoid voltage differences. Therefore, battery thermal management system (BTMS) is a critical role in addressing thermal safety, improving performance, and extending lifetime (Liu et al., 2017; Arora, 2018; Zichen & Changqing, 2021).

BTMS with phase change phenomenon is an impressive way with superior characteristics including high heat absorption capability in lesser volume, isothermally process, simple lightweight and also with noise-free and no-additional power to make reduced carbon footprint batteries for a green environment. Nevertheless, low thermal conductance causes low heat dissipation rates in the medium and leakage issues of kinds of paraffin are two main restrictions for the application of PCM-based cooling strategies. Graphite matrix is a promising approach with high porosity, higher heat transfer surface-to-volume ratio, high thermal conductance, non-reactive nature (chemically), and also surrounding medium to avoid these disadvantages. Therefore, graphite matrix provides abundant highly conductive thermal paths (Mills et al., 2006; Kang et al., 2019) and shape-stabilized encapsulation (Zhang et al., 2021) to dissipate heat rapidly and overcome leakage issues respectively, for PCM medium.

The research on graphite matrix/foam with PCM is presented for battery thermal management as follows: Mills et al. (2006) published the first paper (based on author knowledge) on expanded graphite matrix with PCM for battery cooling. The authors studied thermal conductivity, paraffin mass fraction, and latent heat of fusion of PCM/graphite matrix composites. They reported the potential of the graphite composite with PCM. Kizilel et al. (2008) tested the potential of the graphite matrix composite with PCM compared to conventional active cooling systems. They observed that the cell surface temperature is lower temperatures by graphite-PCM case. Kizilel et al. (2009) performed a CFD study to illustrate the thermal performance of graphite composite with PCM for a cylindrical battery pack. The PCM/graphite matrix helped the battery to achieve a more uniform distribution and to avoid the propagation of a thermal runaway from one cell to the entire pack. Somasundaram et al. (2012) investigated the effect of different discharge rates on PCM/graphite matrix performance by a two-dimensional transient mathematical model. Authors reported that lower temperature values were measured with a graphite matrix composite. Greco et al. (2015) performed a numerical study considering the thermal responses of different configurations of graphite matrix composite. The importance of the mutual effect between latent heat and thermal conductivity was reported. Moreover, outputs show that the graphite matrix bulk density was a key parameter to optimize the graphite composite with PCM. An experimental investigation is carried out to show the effect of melting phase change composite on delaying thermal runaway for a single cell by Wilke et al. (2017). Authors reported that hot spot temperature is diminished by 60 °C, and so thermal runaway is inhibited due to propagation between cells following nail penetration. Jiang et al. (2016) carried out both an experimental and a numerical study for composite PCM-based (Expanded graphite/paraffin slurry) thermal management for li-ion cells under constant current. The thermal conductivity of PCM was enhanced with expanded graphite (EG), and packing in aluminium tubes. The configuration showed higher heat dissipation rates and lower temperature increase rates. However, the authors reported that the temperature gradient in the battery pack was near 12 °C. A similar study (EG/paraffin slurry) was also carried out under constant current by Lv et al. (2016). Wu et al. (2016) fulfilled an experimental study on the effect of copper mesh (CM)-enhanced paraffin (PA)/expanded graphite (EG) composite. To enhance both the thermal conductivity and strength of the proposed arrangement, the copper mesh

acts as a skeleton. As a result, the CM-enhanced PA/EG plate (PCMP) showed a higher heat dissipation rate and uniform temperature profile under constant discharge rates. A heat pipe-assisted PCM/EG-based battery thermal management (BTM) system is investigated with constant discharge currents by [Wu et al. \(2017\)](#). Research on the effect of two high thermal conductivity materials including aluminium and graphite foams, which are saturated with different phase change materials is conducted by [Mallow et al. \(2018\)](#). The authors reported that graphite foams showed superior performance compared to aluminium foams. [Ling et al. \(2018\)](#) performed two different slurries of graphite composites with PCM (graphite-PCM and graphite-PCM-Fumed silica) for battery thermal management. It is reported that the hot spot temperature value of the cell was diminished, and more temperature uniformity was provided with graphite-PCM. A similar study is performed by [Wang et al. \(2018\)](#). [Li et al. \(2018\)](#) extend the investigation with additional silica gel and Al-honeycomb (Al-Hc) components. It was declared by the authors that composite PCM could improve temperature uniformity and reduce the average temperature of the battery. [He et al. \(2019\)](#) proposed a composite PCM with a highly thermal conductive framework of EG/copper foam (CF) for battery thermal management. The results showed that the composite PCM-based battery pack with EG/CF (CPCM-EG/CF) achieves much better cooling and uniform temperature distribution than those without EG/CF or CF under constant discharge rates. A numerical study on the thermal response of the battery module via graphite composite was conducted by [Xin et al. \(2022\)](#). The authors investigated the effect of research parameters including composite PCM thicknesses, graphite mass fractions, and coolant flow directions/velocity/temperatures. [Akula & Balaji \(2022\)](#) carried out both a numerical and an experimental study to illustrate the effect of the proposed PCM-graphite composite slurry with a fin on the thermal management of a battery at constant discharge rates ($> 2C$ -rate). Authors show remarkable enhancement in temperature increase rate/uniformity, thermal conductivity, and thermal capacitance with the addition of 30% expanded graphite (EG). This resulted in lower fin number usage in the heat sink compared to the heat sink without EG. [Yazıcı \(2022b\)](#) conducted an experimental study to test the effect of the various constant discharge currents on a thermal behavior of small-scale battery package. The author presents that the graphite matrix composite with phase change has remarkable outputs, especially, for higher discharge rates.

Researchers have studied experimentally/numerically the effect of graphite composite with PCM for battery cooling under constant discharge rates in the cited literature above. But, there are restricted studies tested under dynamic discharge conditions for cooling strategies with PCM. So, the motivation of this study is to explore the effect of the phase change temperature of graphite composite on the performance of small-scale battery packs under the dynamic/square wave discharge currents. The effect of the melting phenomenon and porous media on the thermal performance of li-ion is also presented comprehensively. To illustrate thermal response, transient temperature profile and thermal camera images are utilized. Moreover, for electrical behaviour, time-dependent energy capacity, discharge capacity and voltage variations are presented. Experimental results are given comparatively with a free-air cooling case to evaluate graphite matrix composite with various melting ranges of PCMs.

2. Material and Methods

2.1. Phase change composite experimental setup and procedure

RT-35 and RT-42 (organic paraffin) supplied from Rubitherm are utilized to store dissipated heat by the Li-ion battery pack. Paraffin is an impressive material with great potential including, high latent heat of fusion, thermal/physical/chemical stability, no phase segregation, non-reactivity, proper compatibility with other materials and safe ([Ahmed et al., 2022](#)). The thermal properties of the paraffin and graphite matrix composites are given in Table 1. Heat flow as a function of the temperature of pure paraffin and graphite matrix composites was measured by Hitachi-7020 (DSC).

Table 1. Thermal properties of materials

Thermo-physical property	RT-35/42	Graphite matrix composite with RT-35	Graphite matrix composite with RT-42
Melting temperature (°C)	37.2/41.4	36.1	40.3
Latent heat (kJ kg ⁻¹)	150/162	144	148
Thermal conductivity (W m ⁻¹ K ⁻¹)	0.2/0.2	7.2	8
Density (kg m ⁻³) (at 25 °C)	860/880	796	730

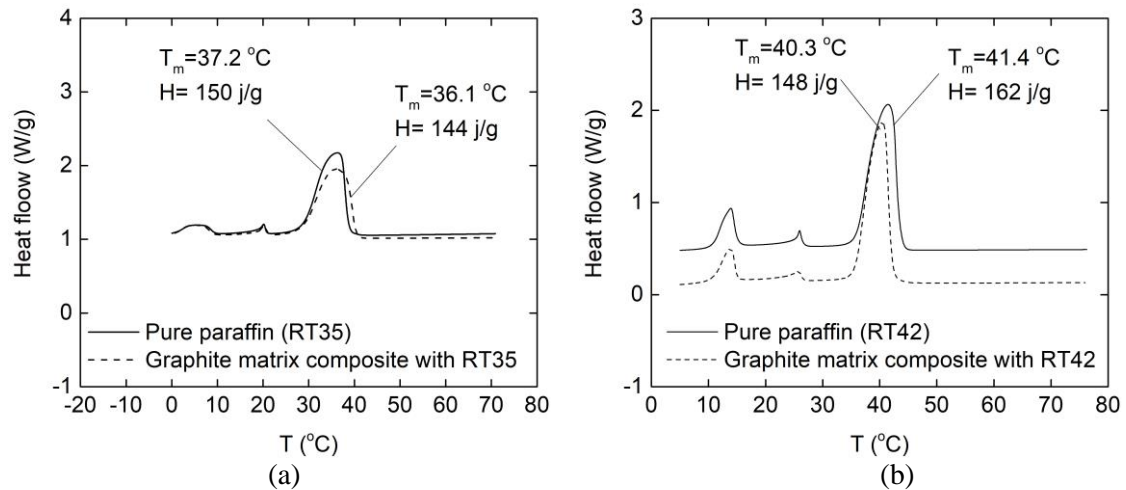


Figure 1. DSC analysis of pure paraffin and graphite composite of (a) RT35 (Yazıcı, 2022a,b) and (b) RT42 (Yazıcı and Saglam, 2021).

To build the graphite matrix, expanded graphite (EG) produced by heat treatment (expansion and exfoliation at 900 - 1 000 °C - 60 seconds) was pressurized in a mould using Instron 3382. The manufacturing process of expanded graphite can be found in detail in the literature (Py et al., 2001; Mills et al., 2006). In this experimental study, expandable graphite with 50 mesh, > %98 purity, and 700 ml g⁻¹ (maximum expansion rate) was provided by Asbury Carbon. Graphite matrix with an overall dimension of 75 mm (Length) x 52 mm (Width) x 60 mm (Height) and bulk density of 75 g l⁻¹ was produced for a small-scale battery pack (3s2p). to obtain a graphite matrix composite with phase change, the graphite matrix was immersed in a liquid paraffin bath (75-80 °C) for about 3-4 hours for saturation. The graphite matrix was saturated with melted paraffin via surface tension and capillarity (Py et al., 2001; Mills et al., 2006). The PCM quantity in the graphite composite with phase change is nearly 103 grams. The paraffin mass fraction is 92% in graphite composite. Transient PCM saturation in the graphite matrix is illustrated in Figure 2. The porosity ratio of the graphite matrix is measured at 85 % considering PCM volume. Impregnation encapsulation provides shape-stabilized PCMs (Zhang et al., 2021) to avoid PCM leakage from the matrix. The leakage test is given in Figure 3. The composite material is put on the paper and heated up to 75 °C for 150 minutes. It is observed that graphite composite with phase change saves its form with a very low leakage rate of 0.41% (0.42 grams) on the paper. This low leakage rate can be expressed by the melting of covered solid PCM on the surface.

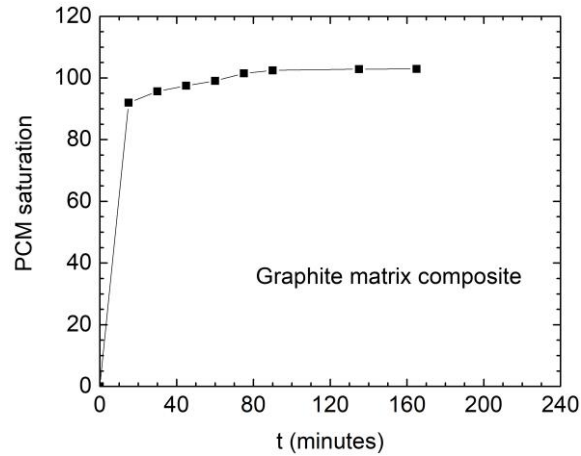


Figure 2. Transient PCM saturation.

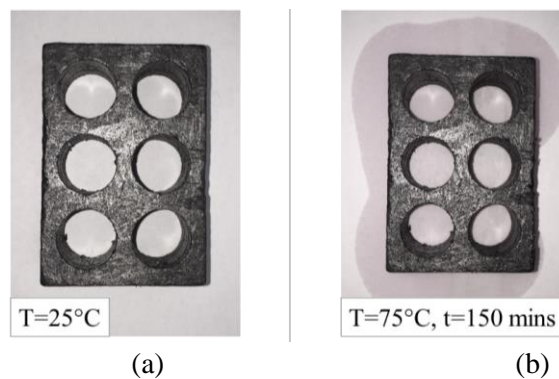


Figure 3. Leakage test: (a) T=25 °C, (b) T=75 °C (Yazıcı, 2022b).

To image structural topology, SEM (Scanning electron microscope, Zeiss EVO LS10) analysis was used. Structural images for the expanded graphite matrix and the graphite matrix composite are shown in Figure 4. Worm-like/vermicular particles are observed on the sample surface image for the graphite matrix (Figure 4a). Moreover, it is shown in Figure 4a that in terms of the overlapping and intersecting of graphite flakes, a honeycomb-like network is developed (Zou et al., 2020). However, some non-interlocking zones between expanded graphite layers (Figure 4a). for graphite matrix composite with phase, it is observed with the surface image of the sample in Figure 4b that the paraffin is impregnated to the matrix, and covers the surface.

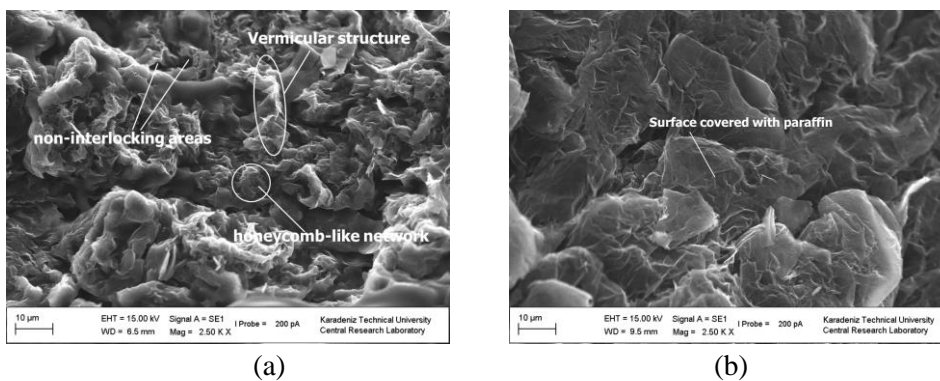
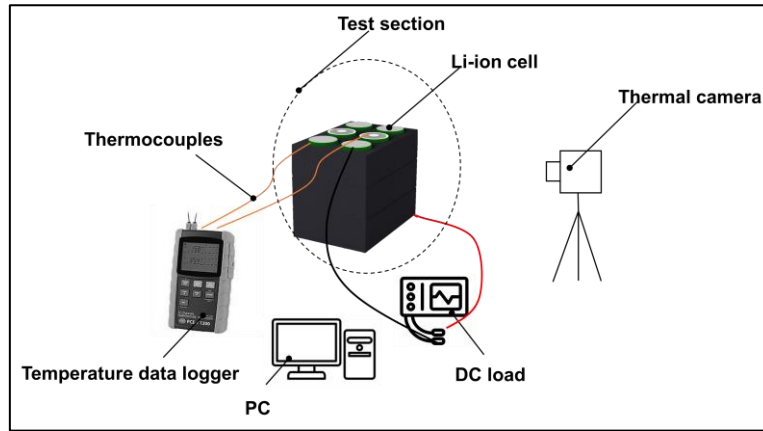


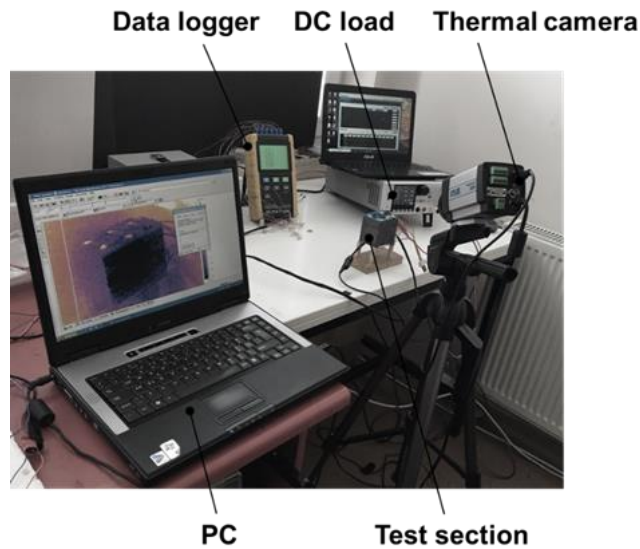
Figure 4. Structural topology images: (a) the graphite matrix and (b) the graphite matrix composite with phase change (RT-35).

2.2. Experimental setup and procedure

The experimental rig is given in Figure 5. It consists of a test section, a DC load, a data logger, a PC, and a thermal camera.



(a)



(b)

Figure 5. Experimental setup: (a) schematic view, (b) photograph.

The test section comprises li-ion cells, nickel sheets for cell connection, terminals, thermocouples and thermal management configurations including free-air cooling (Figure 6a) and graphite matrix composite with phase change (Figures 6b and c). To test the battery package (3s2p) under a dynamic load-the square wave, an electronic DC load (Chroma, CH-63004-150-60) with the accuracy of current of $\pm 0.1\%$ F.S. (± 0.06 amper) is used. The form of the square wave is presented in Figure 7. The dynamic discharge current is set as $I_{\text{maximum}}=16$ A (2.5 C-rate) - $t=16$ seconds and $I_{\text{minimum}}=6.4$ A (1C-rate) - $t=4$ seconds. For electric energy storage, a commercially available li-ion cell of NCR 18650B (Panasonic/Sanyo) is used to form a 3s2p battery pack/module. The cell and battery pack specifications are summarized in Table 2.

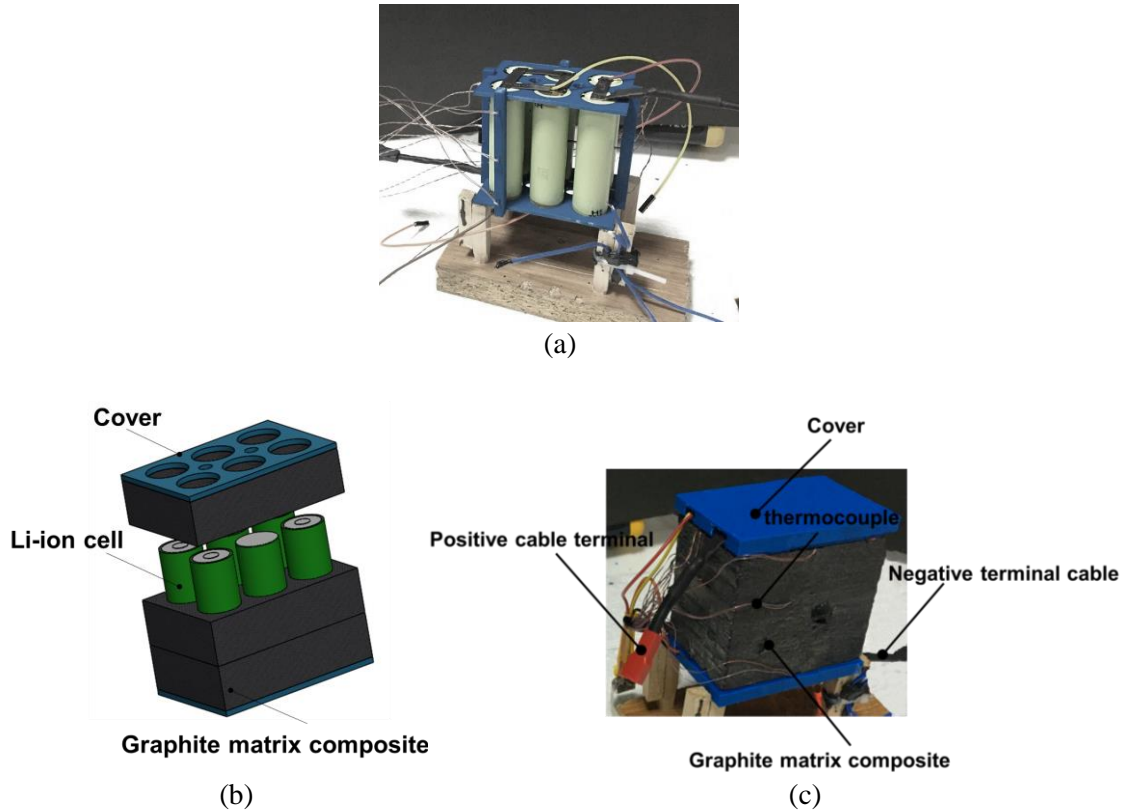


Figure 6. Test section: (a) free-air cooling case, (b) graphite matrix composite / schematic view, (c) phase graphite matrix composite / photograph.

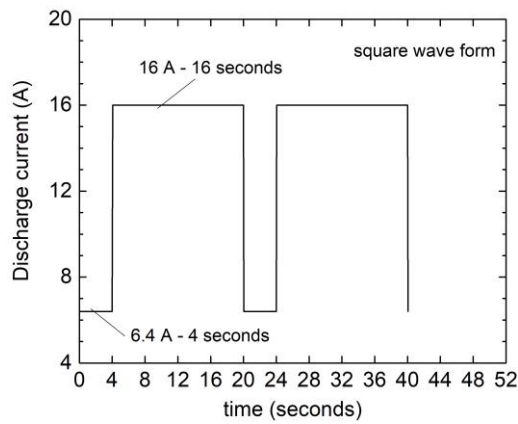


Figure 7. Discharge current variation: square wave form.

Table 2. Li-ion cell and pack specifications

Specification	Cell	Pack
Form factor	1s	3s2p
Capacity nominal (mA h)	3250	6500
Voltage nominal (V)	3.7V	11.1
Specific energy (W h kg ⁻¹)	243	258

Temperature measurement is the key evaluation criterion for the thermal performance of a thermal management system. Therefore, the time-dependent temperature history of the battery package is recorded with six T-type thermocouples (OMEGA brand) with an accuracy of ± 1 °C (or 0.75%). Time-dependent temperature data were recorded with a temperature data logger (PCE-1200) in five seconds intervals. Thermocouple positions/labels on the battery pack are presented in Figure 8. The

thermal camera (Flir, A20) was also used to support thermocouple measurements and also visualize the thermal image of graphite matrix composite with phase change and free-air cooling arrangements.

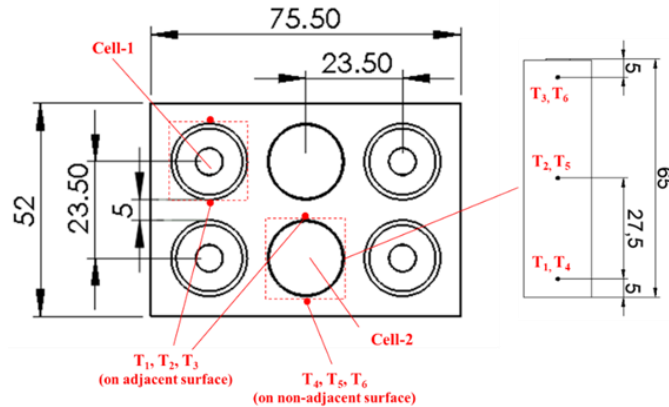


Figure 8. Temperature measurements locations/labels on the li-ion module.

Experiments were conducted in an air-conditioned ambient of 25 °C. Experiments were ended in terms of the limit operating temperature of 55 °C or cut-off voltage of 7.8 V value. It changes depending on which limit is provided first.

3. Results and Discussion

The experimental study is carried out on a small-scale of 3s2p li-ion battery package’s thermal and electrochemical behaviour under dynamic/square wave load for the performance evaluation of graphite matrix composite with phase change material considering two different melting temperatures (RT-35 and RT-42) of PCM. To illustrate the effect of the melting temperature point of graphite composite with phase change, transient temperature distributions and thermal camera images are presented in Figures 9 and 10, respectively. For the electrical performance of the battery pack under dynamic load, the voltage, discharge capacity and energy capacity variation are also shown in Figures 11 - 13. The free air-cooling case is also presented as a reference case in the figures.

Heat transportation in such a porous medium of graphite matrix composite has been considered conduction along highly conductive abundant thermal bridges (Mills et al., 2006; Kang et al., 2019). The advantage of highly conductive thermal bridges of the graphite matrix enhances the process of carrying and storing heat in the phase change phenomenon, which provides the usage of PCM in engineering applications. It should be noted that depending on pore sizes smaller than 10 mm, the natural convection in such a porous medium is suppressed (Kang et al., 2019).

Transient temperature profiles of li-ion cell-1 and cell-2 for free-air cooling and graphite composite are shown in Figure 9. For free-air cooling in Figures 9a and b, heat is not dissipated effectively on the surface of the li-ion cells due to low thermal conductance of $0.025 \text{ W m}^{-1} \cdot \text{K}^{-1}$ (at 25 °C) and low free-convection heat transfer rates. Lower heat dissipation rates from the li-ion surface results in a higher operating temperature of 55 °C, which is critical, in a shorter time of 8.25 minutes. The hot spots are $T_{1/\text{cell-1}}$ and $T_{3/\text{cell-2}}$ for Cell-1 and Cell-2, respectively, because more heat is generated at positive/negative poles. An almost linear increment in temperature is shown in Figures 9a and b. The temperature increase rate is about 3.65 °C/minutes ($T_{3/\text{cell-2}}$). The local temperature point recordings of Cell-2 are higher (4.8 - 9.4 °C) than Cell-1. This temperature difference between cells is associated with the thermal effect of the surrounding li-ion cell-2. It means cell-2 exposes thermal effects more than cell-1 depending on surrounding cells. In addition, temperature values of $T_{1-3/\text{cell-1}}$ and $T_{1-3/\text{cell-2}}$, which are placed on adjacent/ opposing surfaces, are higher compared to $T_{4-6/\text{cell-1}}$ and $T_{4-6/\text{cell-2}}$, respectively, for each cell. This is the result of the thermal effect of opposing/adjacent surfaces to each other. It should be noted that heat loss from the outer/non-adjacent surfaces to the ambient is one of the reasons for this behaviour. So, these result in non-uniform temperature distribution on the battery pack, which causes adverse effects including unbalance of voltage between cells. From Figures

9a and b, the maximum temperature difference ($T_{\max} - T_{\min} = T_{3/\text{cell-2}} - T_{5/\text{cell-1}}$) on the battery pack is about 9.4 °C.

For the graphite composite with different phase changes, the temperature increase rate is lower compared to free-air cooling in Figure 9c-f. With graphite matrix composite with phase changes, a more uniform temperature distribution is observed. This is the result of the highly conductive abundant thermal bridges, which provide effective heat dissipation from the li-ion surface, and also the thermal energy storage capability of PCM. Simultaneously, dissipated heat in graphite matrix composite with phase change is stored with paraffin in the form of sensible and latent heat. Temperature readings report variable temperature increase rates in different periods for graphite matrix composite with RT35 and RT42 in Figures 9c, d, e, and f. The variation of the temperature increase rate is clearer for the other local points, especially, of $T_{4,5,6/\text{cell-1/2}}$ (non-adjacent surfaces) due to the lower temperature increase rate in terms of heat loss. For graphite matrix composite with RT35 and RT42, a steep increase is observed in the first period of $t < 3$ minutes and $t < 6$ minutes of discharging, respectively, due to sensible heat storage. In the following period of $3 < t < 8 - 14$ minutes (for graphite matrix composite with RT35) and $5 < t < 11 - 19$ minutes (for graphite matrix composite with RT42), temperature measurements reach the melting range, and then temperature rise slows down with a positive decrease due to phase transition (for RT35, $T_m = 32 - 38$ °C; for RT42, $T_m = 38 - 43$ °C, Rubitherm datasheet), which provides high energy storage capacity. In the next period of $8 - 14 < t < 19.8$ minutes for graphite matrix composite with RT35 and $11 - 19 < t < 18.67$ minutes for graphite matrix composite with RT42, the rate of temperature rise goes up depending on the completed phase transition phenomenon. To illustrate the thermal behaviour of graphite matrix composite with RT35 and RT42, the temperature increment rate for $T_{3/\text{cell-2}}$ is given in the following as an example. It is shown in Figures 9d and f that a temperature reading ($T_{3/\text{cell-2}}$) increases with 1.5 °C/minutes and 2 °C/minutes rates for RT335 and RT42 cases, respectively, for the first step ($t < 6$ minutes). In the following step ($6 \text{ minutes} < t < 18 \text{ minutes}$), the temperature value increases with the lower rates of 1.24 °C/minutes and 1.02 °C/minutes for RT335 and RT42 cases, respectively. For the RT42 case, the temperature increase rate is half of the first step. For the next step ($t > 18$ minutes), the temperature increase rate is 2.5 °C/minutes with a 100 % increase for the RT35 case, while it is 0.75 °C/minutes with a 25% decrease for the RT42 case. This provides higher temperature values in the package for graphite matrix composite with RT42 in the period of $t < 18$ minutes, while it is observed that lower temperature values are recorded after $t > 18$ minutes. This is the only result of delaying phase change/latent heat storage period depending on the higher melting range for RT42. Because the melting process starts and completes earlier for the RT35 case, temperature values are lower at the initial period due to latent heat and then go up rapidly in terms of sensible heat storage, respectively. However, for the RT42 case, it is shown that some points just reach the upper limit of the melting point. So, rapid temperature increase after the melting process is not achieved by sensible heat. Graphite matrix composite with RT35 gets 3.6-8 °C higher temperature values than the RT42 case at $t > 18$ minutes. For example, at $t = 18$ minutes, temperature values of $T_{3/\text{cell-2}}$ for graphite composite with RT35 and RT42 are 53.4 °C and 49.8 °C, respectively. To present the thermal response of the graphite matrix composite with RT35-RT42, and free-air cooling cases, temperature readings of $T_{3/\text{cell-2}}$ are given at $t = 8$ minutes as follows; 35.6 °C, 38.6 °C and 54.5 °C, respectively. Temperature non-uniformity ($T_{3/\text{cell-2}} - T_{5/\text{cell-1}}$) is decreased to 6.2 °C and 8.7 °C with graphite matrix composite with RT35 and RT42, respectively. The outputs reveal that the operating temperature (at $t = 8$ minutes) is about 34.7 % and 29.2% lower for the graphite matrix composite with RT35 and 42 in comparison to free-air cooling, respectively. Temperature difference (at the end of experiments) is decreased by 34 % and 7 % for the graphite matrix composite with RT35 and 42 compared to free-air cooling, respectively. In addition, safe operating time is 8.25 minutes, 18.67 minutes and 19.83 minutes for free-air cooling, graphite matrix composite with RT42 and RT35, respectively. Graphite matrix composite with RT35 achieved the longest operating time with an increase of 140.4 % and 6.2 % compared to free-air cooling and RT42 case, respectively. The experiments for free-air cooling and graphite composite with RT35 are terminated when the hot spot reaches the limit operating temperature (55 °C), while the experiments are ended with a cut-off voltage (7.8 V) for graphite composite with RT42.

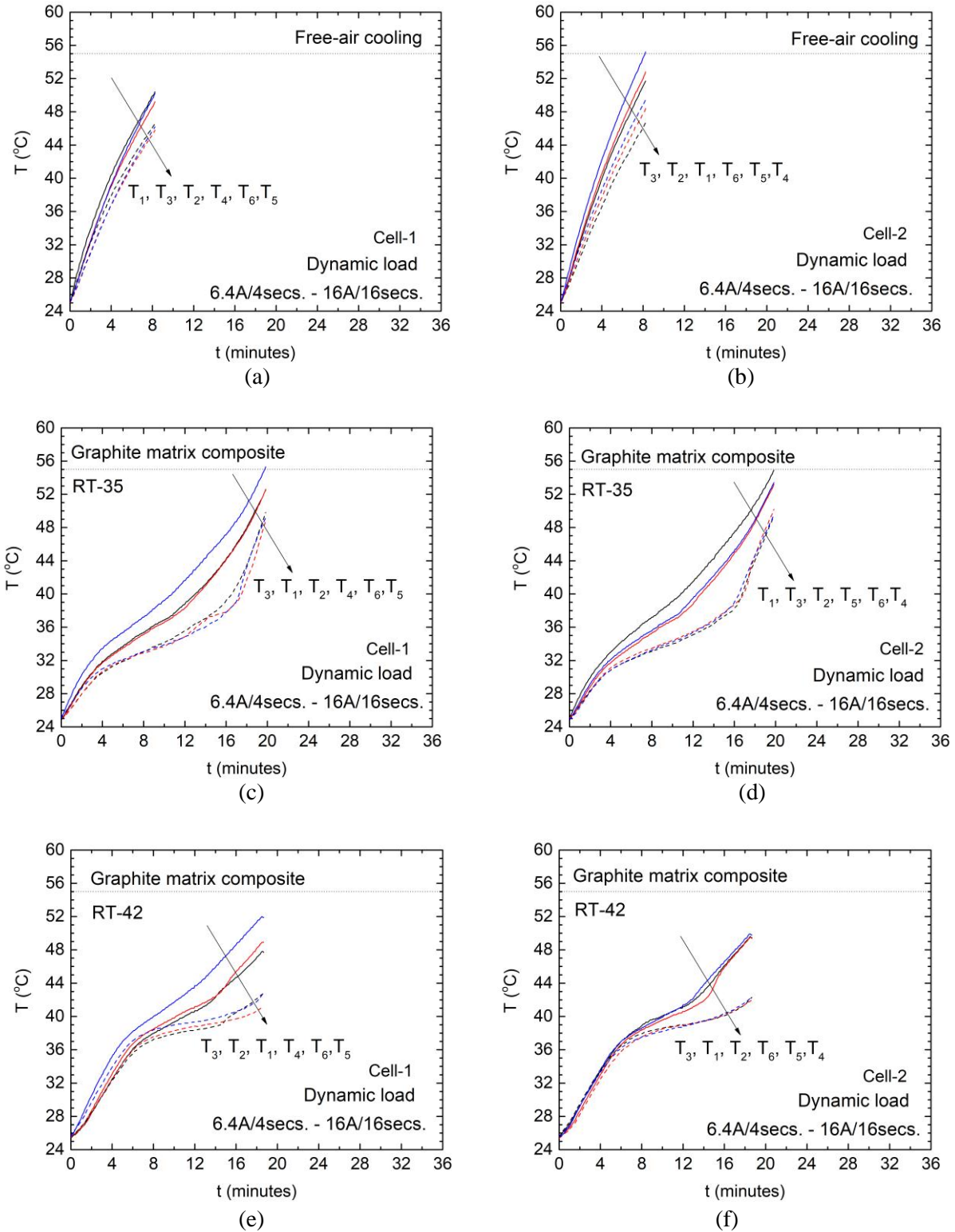


Figure 9. Transient temperature profiles of thermocouple points through the li-ion cell: free-air cooling (a and b), graphite composite; RT-35 (c and d), RT-42 (e and f).

Time-dependent thermal camera images are given in Figure 10. Temperature values show the outer surface temperature of the composite matrix (not directly cell temperature) for the graphite matrix composite with phase change cases, while it shows cell temperature for free-air cooling. Temperature reading increases fast for the free-cooling case. For the graphite composite cases, outer surface temperature values reflect cell temperature values given in Figure 8c - f. In the period of $t < 18$ minutes, the surface temperature of graphite composite with RT42 has higher temperature

reading compared to graphite composite with RT35. Therefore, thermal images support the thermocouple measurement given in Figure 10c - f. Moreover, temperature gradients between the inner (cell temperature) and the outer surface of the package are approximately 9 °C for each case in Figures 10b and c.

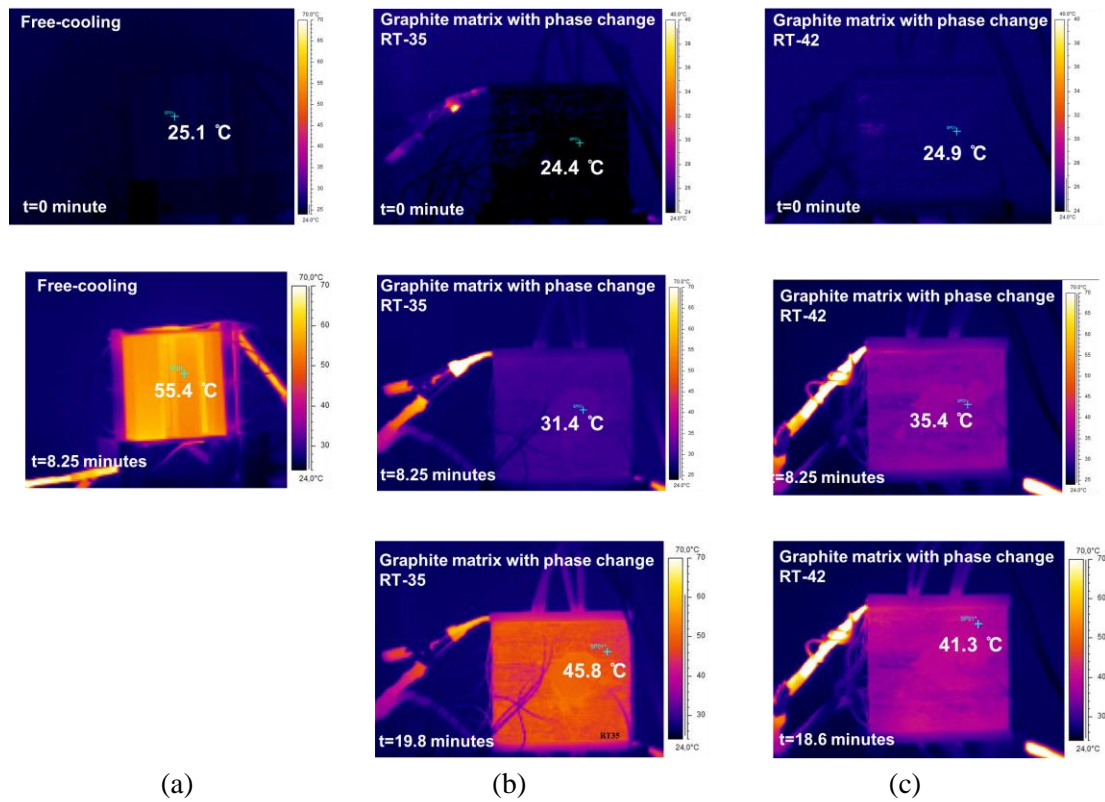


Figure 10. Time-dependent thermal camera photographs: natural convection (a), graphite matrix with RT35 (b) and RT42 (c).

The variation of discharge capacity with voltage (horizontal bottom line) and time depending (horizontal top line/red), transient energy capacity variation, and total energy capacity variation are presented in Figures 11, 12 and 13, respectively, to illustrate the electrical performance of cases. Discharge capacity variation does not decrease continuously during experiments in Figure 11. This is the result of the square wave load. For the highest discharge current of 16 A / 16 seconds, the voltage value decreased higher compared to the moment of the lowest discharge current of 6.4 A / 4 seconds. For example (graphite matrix composite with RT35), at the beginning of the experiment, the voltage decreased from 12.5 V to 11.448 V with the discharge current of 6.4 A / 4 seconds, then, for the next stage with 16 A / 16 seconds, the voltage value decreased 10.248 V suddenly. For the following stage (6.4 A / 4 seconds), the voltage value increases by 11.261 V suddenly in terms of discharge current, which affects ionic movement, and so voltage value variation. Discharge capacity values of free-air cooling and graphite matrix composite with RT 35 and RT42 are 1.93 A h, 4.65 A h and 4.34 A h, respectively. So, the discharge capacity is increased by 141% and 125% for graphite matrix composite with RT35 and RT 42 in comparison to free-air cooling, respectively. Due to the higher temperature increase rate, the discharge capacity is restricted considering the safe temperature (50 °C) for free-air cooling. For graphite composite with RT35, the discharge capacity value is 7% higher compared to RT42 cases depending on the higher operating temperature in safe limits (Figure 9 - 10), which provides higher ionic conductivity of the electrolyte and solid-electrolyte interface and high solid-state diffusion (Yazıcı, 2022a).

Time-dependent energy capacity profiles are presented in Figure 12. Energy capacity, which means power delivered for an hour by the battery, is increasing trend with an increase/decrease profile. Figure 12a - c show that the consumed energy of the battery pack is higher for the graphite matrix composite cases in comparison with the free-air cooling case. In other words, more amount of work is

performed by battery package with graphite matrix composites. This is the result of extended safe operating conditions, in which temperature is one of the key parameters. In addition, the energy capacity reading reaches a higher value in the case of RT35. The total energy capacity values are given for each case with a column chart in Figure 13. The energy capacity delivers 18.5 W h, 37.3 W h and 34.06 W h for free-air cooling and graphite matrix composite with RT35 and 42, respectively. This provides almost 102 % and 84 % more power for an hour for graphite matrix composite with RT35 and RT42 compared to air-cooling. On the other side, 10% more energy capacity for the same initial conditions is achieved by graphite composite with RT35 than RT42 case.

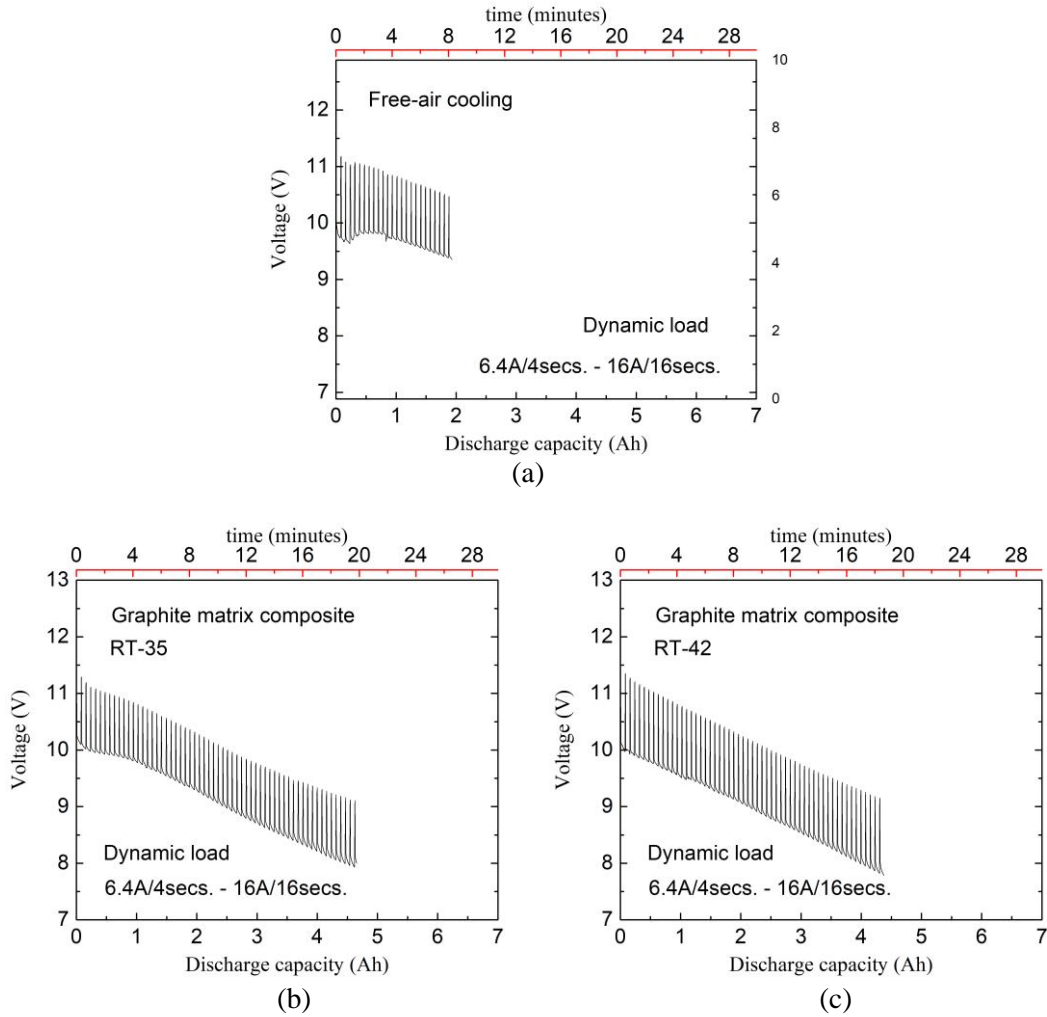


Figure 11. Discharge capacity-voltage-time variation during discharge; (a) free-cooling, graphite matrix with phase change; (b) RT-35, (c) RT-42.

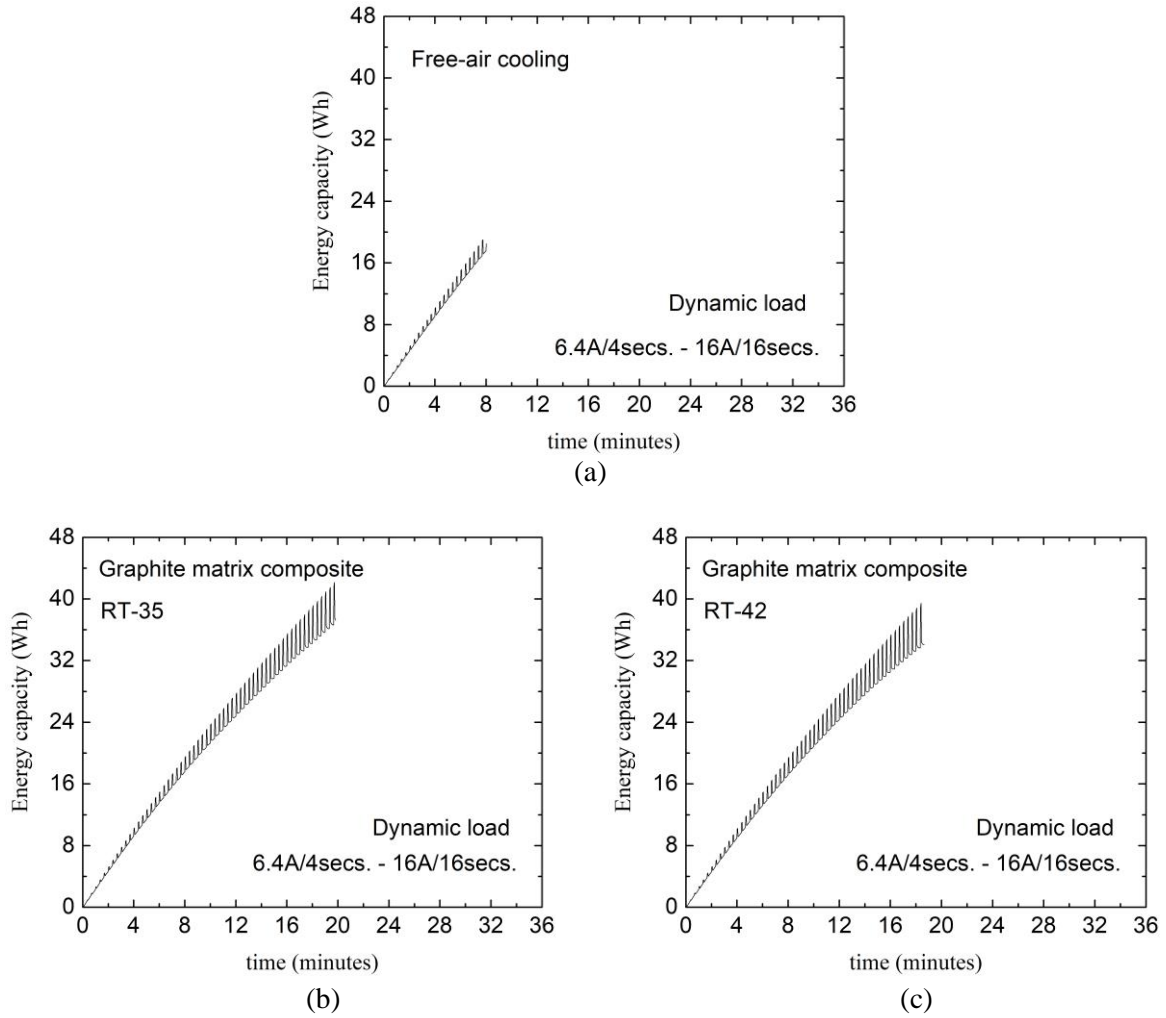


Figure 12. Energy capacity variation: (a) free-cooling, graphite matrix with phase change; (b) RT35, (c) RT42.

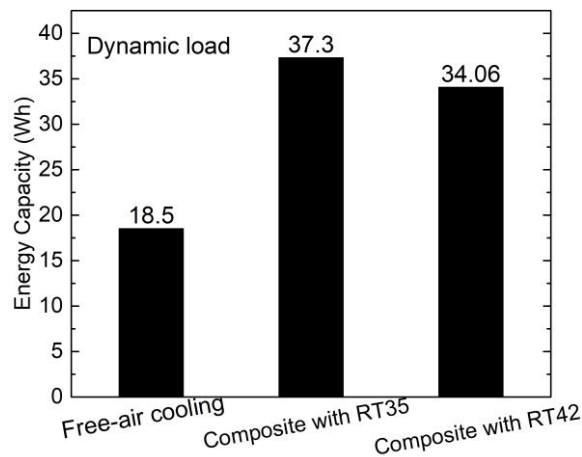


Figure 13. Total energy capacity values for each case.

4. Conclusion

The effect of the phase transition temperature of the graphite composite with phase change on the performance characteristics under square wave load form is explored. Graphite matrix composites

with different phase change points show considerable outputs for the performance of small-scale battery packages. The main outputs are presented below:

- For the graphite composite with RT35 and RT42, the operating temperature is reduced by 34.7 % and 29.2 % compared to free-air cooling, respectively.
- For the graphite composite with RT35 and RT42, the safe operating time increased by 140 % and 126 % compared to free-air cooling, respectively.
- For the graphite composite with RT35 and RT42, the discharge and energy capacity values are augmented by 141 % and 102 %, respectively, in comparison with free-air cooling.
- Graphite composite with RT35 has higher temperature values ($t > 18$ minutes), which provides higher ionic conductivity depending on the phase transition point.
- Graphite composite with RT35 provides 28.7 % better temperature uniformity in the package.
- Graphite matrix composite with RT35 achieved 6.2 % higher operating time in safe limit compared to the RT42 case.
- Graphite matrix composite with RT35 provides 7 % and 10 % higher discharge capacity and energy capacity values in comparison with RT42 cases, respectively.

Acknowledgements

This study was financially supported by TUBITAK TEYDEB with project number 2180111.

References

- Ahmed, S. F., Rafa, N., Mehnaz, T., Ahmed, B., Islam, N., Mofijur, M., Hoang, A. T., & Shafiullah, G. M. (2022). Integration of phase change materials in improving the performance of heating, cooling, and clean energy storage systems: An overview. *Journal of Cleaner Production*, 364, 132639. doi:10.1016/j.jclepro.2022.132639
- Akula, R., & Balaji, C. (2022). Thermal management of 18650 Li-ion battery using novel fins PCM EG composite heat sinks. *Applied Energy*, 316, 119048. doi:10.1016/j.apenergy.2022.119048
- Arora, S. (2018). Selection of thermal management system for modular battery packs of electric vehicles: A review of existing and emerging Technologies. *Journal of Power Sources*, 400, 621 - 640. doi:10.1016/j.jpowsour.2018.08.020
- Greco, A., Jiang, X., & Cao, D. (2015). An investigation of lithium-ion battery thermal management using paraffin/porous-graphite-matrix composite. *Journal of Power Sources*, 278, 50 - 68. doi:10.1016/j.jpowsour.2014.12.027
- He, J., Yang, X., & Zhang, G. (2019). A phase change material with enhanced thermal conductivity and secondary heat dissipation capability by introducing a binary thermal conductive skeleton for battery thermal management. *Applied Thermal Engineering*, 148, 984 - 991. doi:10.1016/j.applthermaleng.2018.11.100
- Jiang, G. W., Huang, J., Fu, Y., Cao, M., & Liu, M. (2016). Thermal optimization of composite phase change material/expanded graphite for Li-Ion battery thermal management. *Applied Thermal Engineering*, 108, 1119 - 1125. doi:10.1016/j.applthermaleng.2016.07.197
- Kang, S., Choi, J. Y., & Choi, S. (2019). Mechanism of heat transfer through porous media of inorganic intumescent coating in cone calorimeter testing. *Polymers*, 11(2), 221. doi:10.3390/polym11020221
- Kizilel, R., Lateef, A., Sabbah, R., Farid, M. M., Selman, J. R., & Al-Hallaj, S. (2008). Passive control of temperature excursion and uniformity in high-energy Li-ion battery packs at high current and ambient temperature. *Journal of Power Sources*, 183(1), 370 - 375. doi:10.1016/j.jpowsour.2008.04.050
- Kizilel, R., Sabbah, R., Selman, J. R., & Al-Hallaj, S. (2009). An alternative cooling system to enhance the safety of Li-ion battery packs. *Journal of Power Sources*, 194, 1105 - 1112. doi:10.1016/j.jpowsour.2009.06.074
- Li, J., Huang, J., & Cao, M. (2018). Properties enhancement of phase-change materials via silica and Al honeycomb panels for the thermal management of LiFeO₄ batteries. *Applied Thermal Engineering*, 131, 660 - 668. doi:10.1016/j.applthermaleng.2017.12.023

- Ling, Z., Wen, X., Zhang, Z., Fang, X., & Gao, X. (2018). Thermal management performance of phase change materials with different thermal conductivities for Li-ion battery packs operated at low temperatures. *Energy*, 144, 977 - 983. doi:10.1016/j.energy.2017.12.098
- Liu, H., Wei, Z., He, W., & Zhao, J. (2017). Thermal issues about Li-ion batteries and recent progress in battery thermal management systems: A review. *Energy Conversion and Management*, 150, 304 - 330. doi:10.1016/j.enconman.2017.08.016
- Lv, Y., Yang, X., Li, X., Zhang, G., Wang, Z., & Yang, C. (2016). Experimental study on a novel battery thermal management technology based on low density polyethylene-enhanced composite phase change materials coupled with low fins. *Applied Energy*, 178, 376 - 382. doi:10.1016/j.apenergy.2016.06.058
- Mallow, A., Abdelaziz, O., & Graham, S. (2018). Thermal charging performance of enhanced phase change material composites for thermal battery design. *International Journal of Thermal Sciences*, 127, 19 - 28. doi:10.1016/j.ijthermalsci.2017.12.027
- Mills, A., Farid, M., Selman, J. R., & Al-Hallaj, S. (2006). Thermal conductivity enhancement of phase change materials using a graphite matrix. *Applied Thermal Engineering*, 26, 1652-1661. doi:10.1016/j.applthermaleng.2005.11.022
- Py, X., Olives, R., & Maurant, S. (2001). Paraffin/porous-graphite-matrix composite as a high and constant power thermal storage material. *International Journal of Heat and Mass Transfer*, 44(14), 2727 - 2737. doi:10.1016/S0017-9310(00)00309-4
- Somasundaram, K., Birgersson, E., & Mujumdar, A. S. (2012). Thermal-electrochemical model for passive thermal management of a spiral-wound lithium-ion battery. *Journal of Power Sources*, 203, 84 - 96. doi:10.1016/j.jpowsour.2011.11.075
- Wang, W., Zhang, X., Xin, C., & Rao, Z. (2018). An experimental study on thermal management of lithium-ion battery packs using an improved passive method. *Applied Thermal Engineering*, 134, 163 - 170. doi:10.1016/j.applthermaleng.2018.02.011
- Wilke, S., Schweitzer, B., Khateeb, S., & Al-Hallaj, S. (2017). Preventing thermal runaway propagation in lithium-ion battery packs using a phase change composite material: An experimental study. *Journal of Power Sources*, 340, 51 - 59. doi:10.1016/j.jpowsour.2016.11.018
- Wu, W., Yang, X., Zhang, G., Ke, X., Wang, Z., Situ, W., Li, X., & Zhang, J. (2016). An experimental study of thermal management system using copper mesh-enhanced composite phase change materials for power battery pack. *Energy*, 113, 909 - 916. doi:10.1016/j.energy.2016.07.119
- Wu, W., Yang, X., Zhang, G., Chen, K., & Wang, S. (2017). Experimental investigation on the thermal performance of heat pipe-assisted phase change material-based battery thermal management system. *Energy Conversion and Management*, 138, 486 - 492. doi:10.1016/j.enconman.2017.02.022
- Xin, Q., Xiao, J., Yang, T., Zhang, H., & Long, X. (2022). Thermal management of lithium-ion batteries under high ambient temperature and rapid discharging using composite PCM and liquid cooling. *Applied Thermal Engineering*, 210, 118230. doi:10.1016/j.applthermaleng.2022.118230
- Yazıcı, M. Y., & Saglam M. (2021). *Thermal management of small-scale Li-Ion battery module using graphite matrix composite with phase change: Effect of phase transition temperature*. 23rd Congress on Thermal Science and Technology with International Participation (ULIBTK 2021), Gaziantep.
- Yazıcı, M. Y. (2022a). The effect of a new design preheating unit integrated to graphite matrix composite with phase change battery thermal management in low-temperature environment: An experimental study. *Thermal Science and Engineering Progress*, 29, 101244. doi:10.1016/j.tsep.2022.101244
- Yazıcı, M. Y. (2022b). Thermal management of small-scale Li-ion battery module using graphite matrix composite with phase change: Effect of discharge rate. *Iğdir Üniversitesi Journal of the Institute of Science and Technology*, 12, 389 - 402. doi:10.21597/jist.952021
- Zhang, S., Feng, D., Shi, L., Wang, L., Jin, Y., Tian, L., Li, Z., Wang, G., Zhao, L., & Yan, Y. (2021). A review of phase change heat transfer in shape-stabilized phase change materials (ss-PCMs) based on porous supports for thermal energy storage. *Renewable and Sustainable Energy Reviews*, 135, 110127. doi:10.1016/j.rser.2020.110127

- Zichen, W., & Changqing, D. (2021). A comprehensive review on thermal management systems for power lithium-ion batteries. *Renewable and Sustainable Energy Reviews*, 139, 110685. doi:10.1016/j.rser.2020.110685
- Zou, T., Liang, X., Wang, S., Gao, X., Zhang, Z., & Fang, Y. (2020). Effect of expanded graphite size on performances of modified CaCl₂·6H₂O phase change material for cold energy storage. *Microporous and Mesoporous Materials*, 305, 110403. doi:10.1016/j.micromeso.2020.110403